ischemic tissues at the acute stage of myocardial infarction (1). Thus, these microenvironmental factors in the host cardiac tissue might not greatly contribute to the therapeutic efficacy of the CSC sheet for the chronic ischemic injury model.

In contrast to CSC sheet transplantation, intramyocardial EPC injection significantly enhanced the improvement in myocardial function only in the ischemic and peri-ischemic endocardium, and not in the epicardium, in a paracrine manner. Urbich et al. reported that soluble factors released by EPCs promote the migration of cardiac-resident progenitor cells, using an in vitro migration assay (31). Thus, we considered that EPCs intramyocardially injected into the ischemic endocardium might promote the host tissue's expression of the angiogenic cytokine SDF-1, consequently enhancing the therapeutic efficacy of CSC sheet transplantation by improving the migration of the transplanted CSCs into the native ischemic myocardium.

The graft rate of transplanted EPCs by intramyocardial injection was lower than that of transplanted CSCs by the cell sheet technique. Transplanted CSCs were uniformly identified in the ischemic epicardium, whereas transplanted EPCs were densely located within the vascular wall of the ischemic and peri-ischemic endocardium. These different graft rates and patterns of transplanted cells might be related to the greater improvement in ESPVR and lower frequency (although not significant) of premature ventricular contraction seen in the animals receiving CSC sheet implantation alone compared with intramyocardial EPC injection alone, as previously described (20,26). One might think that EPCs could be mixed into the CSC sheet to enhance the CSCs' function; however, we have not been able to generate cell sheets from such mixed cultures. In addition, the injection of EPCs into the endocardial area might be important for attracting the migration of CSCs from the surface to the endocardial area.

In this study, contrast echocardiography dissected the improved myocardial perfusion that was seen 8 weeks after cell transplantation in all the cell therapy groups, but not the sham group. It has been shown that myocardial perfusion is impaired in chronic ischemic cardiomyopathy and that improved myocardial perfusion is associated with a suppression of LV remodeling (8). These findings indicate that the therapeutic efficacy in all the cell therapy groups might have been mainly attributable to the suppressive effects on LV remodeling. Consistent with this idea, multidetector CT showed that the increased rate of EDV between before and 8 weeks after treatment was less than 20% in all the cell therapy groups, but not in the sham group. On the other hand, invasive hemodynamic assessment using a conductance catheter also showed that CSC sheet implantation or the intramyocardial injection of EPCs significantly improved measures of LV diastolic functions, such as τ and EDP, compared with the sham operation. Previous reports demonstrated that the stiffness of the infarcted myocardium plays an important role in the postinfarction remodeling process (25). Thus, the different types of cell therapy we used may have had a softening effect on the scar tissue by increasing the cellularity, leading to a more pliable scar and less global cardiac remodeling.

In this study, in vivo CSC sheet implantation or concomitant EPC injection rarely induced the differentiation of transplanted CSCs into cardiomyogenic or vasculogenic lineages. Instead, all of the cardiac protein-expressing transplanted cells arose from fusion with existing myocytes or endothelial cells. Several lines of evidence support the idea that differentiation potential can be altered by differences in the severity of the pretreated infarct, as well as the timing of cell transplantation (20,21). In particular, Matsuura et al. reported that in viable ischemic tissues with existing cardiomyocytes, CSCs are likely to differentiate into myocytes or vascular cells via a cell fusion-dependent mechanism (20). Our layer-specific regional functional analysis by strain echocardiography identified residual viability in the ischemic area just before the cell therapies, and these conditions might have limited the differentiation potential of the CSC sheet in vivo and the ability of additional EPC injection to promote the differentiation of CSCs into the cardiomyogenic or vasculogenic lineages.

A potential limitation of this study is that the human c-kit-positive CSCs were obtained from a single donor. However, the isolation and culture methods for the primary c-kit-positive CSCs used in this study were previously established to yield CSCs of consistent functionality regardless of the donor (30). The findings of this study are therefore likely to be consistent with those obtained using CSCs from a different donor. In addition, although the swine were immunosuppressed by a previously reported regimen (15), xenogeneic cell transplantation might limit or exaggerate the therapeutic efficacy of the treatment. However, our analysis of layer-specific regional function clearly demonstrated the previously undescribed therapeutic benefit that additional EPC injection improves the CSC sheet therapy for the swine ischemic injury model.

In summary, CSC transplantation by the cell sheet technique prevented LV remodeling, through increased neovascularization and reduced fibrosis in a paracrine manner, and consequently improved the global LV function, and these effects were further enhanced by combination therapy with EPC injection. Our layer-specific strain analysis revealed that CSC sheet implantation improved regional wall motion in the epicardium, but not the endocardium. However, concomitant EPC transplantation significantly enhanced the therapeutic potential of CSC sheet

therapy in the endocardium. Concomitant EPC injection promoted migration of transplanted CSCs into the host myocardium, which might contribute to enhancement of functional recovery in the endocardium by the combination therapy. The combination of CSC sheet implantation and intramyocardial EPC injection may represent a promising strategy for ischemic cardiomyopathy.

ACKNOWLEDGMENTS: We thank Mr. Tsuyoshi Ishikawa for cell culturing and Mr. Shigeru Matsumi for excellent technical assistance for the surgery and care of the animals. This study was financially supported by a Grant-in-Aid of Scientific Research (08062134) from the Ministry of Health, Labour, and Welfare of Japan. Mr. Akima Harada is a full-time employee of CellSeed Inc., Japan. Mr. Tatsuya Shimizu and Mr. Teruo Okano are members of the scientific advisory board of CellSeed Inc., Japan. The authors declare no additional conflicts of interest.

REFERENCES

1. Abbott, J. D.; Huang, Y.; Liu, D.; Hickey, R.; Krause, D. S.; Giordano, F. J. Stromal cell-derived factor-1alpha plays a critical role in stem cell recruitment to the heart after myocardial infarction but is not sufficient to induce homing in the absence of injury. Circulation 110(21):3300–3305; 2004.
2. Adamu, U.; Schmitz, F.; Becker, M.; Kelm, M.; Hoffmann, R. Advanced speckle tracking echocardiography allowing a three-myocardial layer-specific analysis of deformation parameters. Eur. J. Echocardiogr. 10(2):303–308; 2009.
3. Becker, M.; Altiok, E.; Lente, C.; Otten, S.; Friedman, Z.; Adam, D.; Hoffmann, R.; Koos, R.; Krombach, G.; Marx, N. Layer-specific analysis of myocardial function for accurate prediction of reversible ischaemic dysfunction in intermediate viability defined by contrast-enhanced MRI. Heart 97(9):748–756; 2011.
4. Becker, M.; Ocklenburg, C.; Altiok, E.; Futing, A.; Balzer, J.; Krombach, G.; Lysyansky, M.; Kuhl, H.; Krings, R.; Kelm, M.; Hoffmann, R. Impact of infarct transmurality on layer-specific impairment of myocardial function: Amyocardial deformation imaging study. Eur.Heart J. 30(12):1467–1476; 2009.
5. Bel, A.; Planat-Bernard, V.; Saito, A.; Bonnevie, L.; Bellamy, V.; Sabbah, L.; Bellabas, L.; Brinon, B.; Vanneaux, V.; Pradeau, P.; Peyrard, S.; Larghero, J.; Pouly, J.; Binder, P.; Garcia, S.; Shimizu, T.; Sawa, Y.; Okano, T.; Bruneval, P.; Desnos, M.; Hagege, A. A.; Casteilla, L.; Puceat, M.; Menasche, P. Composite cell sheets: A further step toward safe and effective myocardial regeneration by cardiac progenitors derived from embryonic stem cells. Circulation 122(11 Suppl):S118–123; 2010.
6. Bolli, R.; Chugh, A. R.; D'Amario, D.; Loughran, J. H.; Stoddard, M. F.; Ikram, S.; Beache, G. M.; Wagner, S. G.; Leri, A.; Hosoda, T.; Sanada, F.; Elmore, J. B.; Goichberg, P.; Cappetta, D.; Solankhi, N. K.; Fahsah, I.; Rokosh D. G.; Slaughter, M. S.; Kajstula, J.; Anversa, P. Cardiac stem cells in patients with ischaemic cardiomyopathy (SCIPIO): Initial results of a randomised phase 1 trial. Lancet 378 (9806):1847–1857; 2011.
7. Dib, N.; Khawaja, H.; Varner, S.; McCarthy, M.; Campbell, A. Cell therapy for cardiovascular disease: A comparison of methods of delivery. J. Cardiovasc. Transl. Res. 4(2):177–181; 2011.
8. Galiuto, L.; Garramone, B.; Scara, A.; Rebuzzi, A. G.; Crea, F.; La Torre, G.; Funaro, S.; Madonna, M.; Fedele, F.; Agati, L. The extent of microvascular damage during myocardial contrast echocardiography is superior to other known indexes of post-infarct reperfusion in predicting left ventricular remodeling: Results of the multicenter AMICI study. J. Am. Coll. Cardiol. 51(5):552–559; 2008.
9. Hosoda, T.; Zheng, H.; Cabral-da-Silva, M.; Sanada, F.; Ide-Iwata, N.; Ogorek, B.; Ferreira-Martins, J.; Arranto, C.; D'Amario, D.; del Monte, F.; Urbanek, K.; D'Alessandro, D. A.; Michler R. E.; Anversa, P.; Rota, M.; Kajstura, J.; Leri, A. Human cardiac stem cell differentiation is regulated by a mircrine mechanism. Circulation 123(12):1287–1296; 2011.
10. Imanishi, Y.; Miyagawa, S.; Meaeda, N.; Fukushima, S.; Kitagawa-Sakakida, S.; Daimon, T.; Hirata, A.; Shimizu, T.; Okano, T.; Shimomura, I.; Sawa, Y. Induced adipocyte cell-sheet ameliorates cardiac dysfunction in a mouse myocardial infarction model: A novel drug delivery system for heart failure. Circulation 124(suppl 1):S10–S17; 2011.
11. Iwasaki, H.; Kawamoto, A.; Ishikawa, M.; Oyamada, A.; Nakamori, S.; Nishimura, H.; Sadamoto, K.; Horii, M.; Matsumoto, T.; Murasawa, S.; Shibata, T.; Suehiro, S.; Asahara, T. Dose-dependent contribution of CD34-positive cell transplantation to concurrent vasculogenesis and cardiomyogenesis for functional regenerative recovery after myocardial infarction. Circulation 113(10):1311–1325; 2006.
12. Kawaguchi, N.; Smith, A. J.; Waring, C. D.; Hasan, M. K.; Miyamoto, S.; Matsuoka, R.; Ellison, G. M. c-kit^{pos} GATA-4 high rat cardiac stem cells foster adult cardiomyocyte survival through IGF-1 paracrine signalling. PloS One 5(12):e14297; 2010.
13. Kawamoto, A.; Iwasaki, H.; Kusano, K.; Murayama, T.; Oyamada, A.; Silver, M.; Hulbert, C.; Gavin, M.; Hanley, A.; Ma, H.; Kearney, M.; Zak, V.; Asahara, T.; Losordo, D. W. CD34-positive cells exhibit increased potency and safety for therapeutic neovascularization after myocardial infarction compared with total mononuclear cells. Circulation 114(20):2163–2169; 2006.
14. Kempny, A.; Diller, G. P.; Kaleschke, G.; Orwat, S.; Funke, A.; Radke, R.; Schmidt, R.; Kerckhoff, G.; Ghezelbash, F.; Rukosujew, A.; Reinecke, H.; Scheld, H. H.; Baumgartner, H. Longitudinal left ventricular 2D strain is superior to ejection fraction in predicting myocardial recovery and symptomatic improvement after aortic valve implantation. Int. J. Cardiol. 167(5):2239–2243; 2013.
15. Kim, B. O.; Tian, H.; Prasongsukarn, K.; Wu, J.; Angoulvant, D.; Wnendt, S.; Muhs, A.; Spitkovsky, D.; Li, R. K. Cell transplantation improves ventricular function after a myocardial infarction: A preclinical study of human unrestricted somatic stem cells in a porcine model. Circulation 112(9 Suppl):I96–104; 2005.
16. Kobayashi, H.; Shimizu, T.; Yamato, M.; Tono, K.; Masuda, H.; Asahara, T.; Kasanuki, H.; Okano, T. Fibroblast sheets co-cultured with endothelial progenitor cells improve cardiac function of infarcted hearts. J. Artif. Organs 11(3):141–147; 2008.
17. Li, N.; Lu, X.; Zhao, X.; Xiang, F. L.; Xenocostas, A.; Karmazyn, M.; Feng, Q. Endothelial nitric oxide synthase promotes bone marrow stromal cell migration to the ischemic myocardium via upregulation of stromal cell-derived factor-1alpha. Stem Cells 27(4):961–970; 2009.

18. Limana, F.; Zacheo, A.; Mocini, D.; Mangoni, A.; Borsellino, G.; Diamantini, A.; De Mori, R.; Battistini, L.; Vigna, E.; Santini, M.; Loiaconi, V.; Pompilio, G.; Germani, A.; Capogrossi, M. C. Identification of myocardial and vascular precursor cells in human and mouse epicardium. Circ. Res. 101(12):1255–1265; 2007.
19. Makkar, R. R.; Smith, R. R.; Cheng, K.; Malliaras, K.; Thomson, L. E.; Berman, D.; Czer, L. S.; Marban, L.; Mendizabal, A.; Johnston, P. V.; Russell, S. D.; Schuleri, K. H.; Lardo, A. C.; Gerstenblith, G.; Marban, E. Intracoronary cardiosphere-derived cells for heart regeneration after myocardial infarction (CADUCEUS): A prospective, randomised phase 1 trial. Lancet 379(9819):895–904; 2012.
20. Matsuura, K.; Honda, A.; Nagai, T.; Fukushima, N.; Iwanaga, K.; Tokunaga, M.; Shimizu, T.; Okano, T.; Kasanuki, H.; Hagiwara, N.;Komuro, I. Transplantation of cardiac progenitor cells ameliorates cardiac dysfunction after myocardial infarction in mice. J. Clin. Invest. 119:2204–2217; 2009.
21. Matsuura, K.; Wada, H.; Nagai, T.; Iijima, Y.; Minamino, T.; Sano, M.; Akazawa, H.; Molkentin, J. D.; Kasanuki, H.; Komuro, I. Cardiomyocytes fuse with surrounding noncardiomyocytes and reenter the cell cycle. J. Cell Biol. 167(2):351–363; 2004.
22. Meyer, G. P.; Wollert, K. C.; Lotz, J.; Steffens, J.; Lippolt, P.; Fichtner, S.; Hecker, H.; Schaefer, A.; Arseniev, L.; Hertenstein, B.; Ganser, A.; Drexler, H. Intracoronary bone marrow cell transfer after myocardial infarction: Eighteen months' follow-up data from the randomized, controlled BOOST (Bone marrOw transfer to enhance ST-elevation infarct regeneration) trial. Circulation 113(10):1287–1294; 2006.
23. Miyagawa, S.; Saito, A.; Sakaguchi, T.; Yoshikawa, Y.; Yamauchi, T.; Imanishi, Y.; Kawaguchi, N.; Teramoto, N.; Matsuura, N.; Iida, H.; Shimizu, T.; Okano, T.; Sawa, Y. Impaired myocardium regeneration with skeletal cell sheets--A preclinical trial for tissue-engineered regeneration therapy. Transplantation 90(4):364–372; 2010.
24. Russell, J. L.; Goetsch, S. C.; Gaiano, N. R.; Hill, J. A.; Olson, E. N.; Schneider, J. W. A dynamic notch injury response activates epicardium and contributes to fibrosis repair. Circ. Res. 108(1):51–59; 2011.
25. Schneider, C.; Jaquet, K.; Geidel, S.; Rau, T.; Malisius, R.; Boczor, S.; Zienkiewicz, T.; Kuck, K. H.; Krause, K. Transplantation of bone marrow-derived stem cells improves myocardial diastolic function: Strain rate imaging in a model of hibernating myocardium. J. Am. Soc. Echocardiogr. 22(10):1180–1189; 2009.
26. Sekine, H.; Shimizu, T.; Dobashi, I.; Matsuura, K.; Hagiwara, N.; Takahashi, M.; Kobayashi, E.; Yamato, M.; Okano, T. Cardiac cell sheet transplantation improves damaged heart function via superior cell survival in comparison with dissociated cell injection. Tissue Eng. Part A 17(23–24):2973–2980; 2011.
27. Shimizu, T.; Sekine, H.; Yamato, M.; Okano, T. Cell sheet-based myocardial tissue engineering: New hope for damaged heart rescue. Curr. Pharm. Design 15(24):2807–2814; 2009.
28. Son, B. R.; Marquez-Curtis, L. A.; Kucia, M.; Wysoczynski, M.; Turner, A. R.; Ratajczak, J.; Ratajczak, M. Z.; Janowska-Wieczorek, A. Migration of bone marrow and cord blood mesenchymal stem cells in vitro is regulated by stromal-derived factor-1-CXCR4 and hepatocyte growth factor-c-met axes and involves matrix metalloproteinases. Stem Cells 24(5):1254–1264; 2006.
29. Tang, J. M.; Wang, J. N.; Zhang, L.; Zheng, F.; Yang, J. Y.; Kong, X.; Guo, L. Y.; Chen, L.; Huang, Y. Z.; Wan, Y.; Chen, S. Y. VEGF/SDF-1 promotes cardiac stem cell mobilization and myocardial repair in the infarcted heart. Cardiovasc. Res. 91(3):402–411; 2011.
30. Tang, X. L.; Rokosh, G.; Sanganalmath, S. K.; Yuan, F.; Sato, H.; Mu, J.; Dai, S.; Li, C.; Chen, N.; Peng, Y.; Dawn, B.; Hunt, G.; Leri, A.; Kajstura, J.; Tiwari, S.; Shirk, G.; Anversa, P.; Bolli, R. Intracoronary administration of cardiac progenitor cells alleviates left ventricular dysfunction in rats with a 30-day-old infarction. Circulation 121(2): 293–305; 2010.
31. Urbich, C.; Aicher, A.; Heeschen, C.; Dernbach, E.; Hofmann, W. K.; Zeiher, A. M.; Dimmeler, S. Soluble factors released by endothelial progenitor cells promote migration of endothelial cells and cardiac resident progenitor cells. J. Mol. Cell. Cardiol. 39(5):733–742; 2005.
32. Wollert, K. C.; Meyer, G. P.; Lotz, J.; Ringes-Lichtenberg, S.; Lippolt, P.; Breidenbach, C.; Fichtner, S.; Korte, T.; Hornig, B.; Messinger, D.; Arseniev, L.; Hertenstein, B.; Ganser, A.; Drexler, H. Intracoronary autologous bone-marrow cell transfer after myocardial infarction: The BOOST randomised controlled clinical trial. Lancet 364(9429): 141–148; 2004.
33. Zakharova, L.; Mastroeni, D.; Mutlu, N.; Molina, M.; Goldman, S.; Diethrich, E.; Gaballa, M. A. Transplantation of cardiac progenitor cell sheet onto infarcted heart promotes cardiogenesis and improves function. Cardiovasc. Res. 87(1):40–49; 2010.
34. Zhou, B.; Ma, Q.; Rajagopal, S.; Wu, S. M.; Domian, I.; Rivera-Feliciano, J.; Jiang, D.; von Gise, A.; Ikeda, S.; Chien, K. R.; Pu, W. T. Epicardial progenitors contribute to the cardiomyocyte lineage in the developing heart. Nature 454(7200):109–113; 2008.

Advance Publication by-J-STAGE

Circulation Journal
Official Journal of the Japanese Circulation Society
http://www.j-circ.or.jp

Targeted Delivery of Adipocytokines Into the Heart by Induced Adipocyte Cell-Sheet Transplantation Yields Immune Tolerance and Functional Recovery in Autoimmune-Associated Myocarditis in Rats

Sokichi Kamata, MD, PhD; Shigeru Miyagawa, MD, PhD; Satsuki Fukushima, MD, PhD; Yukiko Imanishi, PhD; Atsuhiro Saito, PhD; Norikazu Maeda, MD, PhD; Iichiro Shimomura, MD, PhD; Yoshiki Sawa, MD, PhD

Background: Clinical prognosis is critically poor in fulminant myocarditis, while it's initiation or progression is fated, in part, by T cell-mediated autoimmunity. Adiponectin (APN) and associated adipokines were shown to be immune tolerance inducers, although the clinically relevant delivery method into target pathologies is under debate. Whether the cell sheet-based delivery system of adipokines might induce immune tolerance and functional recovery in experimental autoimmune myocarditis (EAM) was tested.

Methods and Results: Scaffold-free-induced adipocyte cell-sheet (iACS) was generated by differentiating adipose tissue-derived syngeneic stromal vascular-fraction cells into adipocytes on temperature-responsive dishes. Rats with EAM underwent iACS implantation or sham operation. Supernatants of iACS contained a high level of APN and hepatocyte growth factor (HGF), and reduced proliferation of CD4-positive T cells in vitro. Immunohistolabelling showed that the iACS implantation elevated the levels of APN and HGF in the myocardium compared to the sham operation, which attenuated the immunological response by inhibiting CD68-positive macropharges and CD4-positive T-cells and activating Foxp3-positive regulatory T cells. Consequently, left ventricular ejection fraction was significantly greater after the iACS implantation than after the sham operation, in association with less collagen accumulation.

Conclusions: The targeted delivery of adipokines using tissue-engineered iACS ameliorated cardiac performance of the EAM rat model via effector T cell suppression and induction of immune tolerance. These findings might suggest a potential of this tissue-engineered drug delivery system in treating fulminant myocarditis in the clinical setting.

Key Words: Adiponectin; Inflammation; Myocarditis; Transplantation

Fulminant myocarditis often follows a rapidly deteriorating course, leading to severe cardiac dysfunction. Efficacy of fast-track immunoglobulin and steroid therapies has been reported,[1] but these treatments are not fully established. Although the pathogenesis of fulminant myocarditis is not fully understood, an autoimmune response against myocardial components has been suggested to play an important role in its progression, consequently leading to end-stage heart failure.[1,2] Interferon (IFN)γ-producing T helper (Th)1 cells and interleukin (IL)17-producing Th17 cells are reported to be key regulators of the autoimmune response, as they activate macrophages in the cardiac tissues to trigger inflammation and inhibit regulatory T cells.[2,3] Strategies for ameliorating the immune response and/or augmenting immune tolerance are therefore under development for treating fulminant myocarditis.

Editorial p????

Fat tissue functions as a type of endocrine organ by secreting its produced cytokines and adipokines, which have pro-inflammatory and anti-inflammatory activities. Adiponectin

Received July 31, 2014; revised manuscript received September 13, 2014; accepted September 24, 2014; released online November 5, 2014 Time for primary review: 19 days

Department of Cardiovascular Surgery (S.K., S.M., S.F., Y.I., A.S., Y.S.), Department of Metabolic Medicine (N.M., I.S.), Osaka University Graduate School of Medicine, Suita, Japan

Mailing address: Yoshiki Sawa, MD, PhD, Department of Cardiovascular Surgery, Osaka University Graduate School of Medicine, 2-2 Yamadaoka, Suita 565-0871, Japan. E-mail: sawa-p@surg1.med.osaka-u.ac.jp

ISSN-1346-9843 doi:10.1253/circj.CJ-14-0840

All rights are reserved to the Japanese Circulation Society. For permissions, please e-mail: cj@j-circ.or.jp

(APN) is an adipokine with strong anti-inflammatory properties and has been suggested to play a protective role in the acute phase of myocarditis in humans.[4,5] Importantly, it has been known that APN is downregulated in a variety of clinical conditions or critical illnesses, such as obesity, type 2 diabetes, and coronary artery disease.[6] In addition, hepatocyte growth factor (HGF), another known anti-inflammatory adipokine, was reported to induce immune tolerance and functional recovery by use of an in vivo transfection technique in experimental autoimmune myocarditis (EAM).[7,8] However, no clinically relevant method for the efficient delivery of APN or HGF into the heart has been well established for treating fulminant myocarditis.

We previously developed the epicardial transplantation of scaffold-free-induced adipocyte cell-sheet (iACS) method, and recently showed that iACS can constitutively deliver a variety of cardioprotective factors, including APN and HGF, to the heart in mice subjected to acute myocardial infarction.[9] Importantly, iACS is generated from adipose tissue-derived stromal vascular fraction (SVF) cells that are isolated from the subcutaneous fat tissue without gene modification, which is promising for the potential use of this method in clinical settings.

We hypothesized that iACS transplantation into the heart might induce immune tolerance and functional recovery in autoimmune-associated myocarditis. Here we examined the biological and functional effects of this method as a drug-delivery system using an EAM rat model. Immunoinhibitory effects of pivotal paracrine factors, such as APN and HGF, on dendritic and effector T cells were also analyzed in vivo and in vitro. In addition, we generated a non-defferentiating SVF cell-sheet (SVFCS) and showed that both the iACS and SVFCS produce a similarly great amount of anti-inflammatory adipokines, including HGF; however, differentiated iACS but not SVFCS was able to secrete a large amount of APN. Therefore, for the purpose of examining the additional effect of APN on EAM, we compared the therapeutic effects of iACS implantation with those of SVFCS implantation.

Methods

Animals

All animal studies were carried out under approval of the institutional ethics committee. This investigation conforms to the Principles of Laboratory Animal Care formulated by the National Society for Medical Research and the Guide for the Care and Use of Laboratory Animals (US National Institutes of Health Publication No. 85-23, revised 1996).

Preparation of SVFCS and iACS

Each iACS was prepared as previously described.[9] Briefly, SVF cells isolated from inguinal adipose tissue were cultured on 35-mm thermo-responsive dishes (CellSeed, Tokyo, Japan), at 2×10^6 cells per dish, to generate each scaffold-free SVFCS. Each iACS was generated by adding 10 mg/ml insulin, 2 mmol/L dexamethasone, 5 mmol/L pioglitazone, and 125 mmol/L isobutylmethylxanthine (Sigma-Aldrich, St Louis, MO, USA) to the SVFCS for 2 days. The medium was then refreshed and the cultures incubated for 5 more days at 37°C. The iACS spontaneously detached from the surface when placed in a 20°C refrigerator.

Generation of the Rat Myocarditis Model and Cell-Sheet Transplantation

Purified porcine cardiac myosin (Sigma-Aldrich) was dissolved in 0.01 mol/L phosphate-buffered saline and emulsified with an equal volume of complete Freund's adjuvant (Difco Laboratories, Detroit, MI, USA). On days 0 and 7, 0.2 ml of the emulsion, which yielded an immunizing dose of 1.0 mg cardiac myosin per rat, was injected subcutaneously into the footpad of male Lewis rats (7 weeks old, 200–250 g).[2] Following the second injection, the rats were randomly assigned to 3 groups and subjected to a thoracotomy and: (1) a sham operation (Sham group; n=58) or transplantation onto the anterior surface of the heart of; (2) 3-layered SVFCS (SVFCS group; n=54); or (3) 3-layered iACS (iACS group; n=58).

Echocardiography and Conductance Catheter

Serial transthoracic echocardiography was performed under inhaled anesthesia with isoflurane (1.5%, 1 L/min; Mylan, Pittsburgh, PA, USA). Two-dimensional short-axis images at the basal, mid, and apical levels were acquired to calculate the left ventricular (LV) ejection fraction (EF) and regional wall motion index (RWMI).[10]

Pressure-volume (P-V) cardiac catheterization was performed after median sternotomy, by inserting a conductance catheter (Unique Medical, Tokyo, Japan) and a Micro Tip catheter transducer (SPR-671; Millar Instrument, Houston, TX, USA) into the LV cavity. The P-V loop data under stable hemodynamics or inferior vena cava occlusion were analyzed with Integral 3 software (Unique Medical).

CD4-Positive T-Cell Proliferation Assay

CD4-positive T cells and antigen-presenting dendritic cells were isolated from the spleen of EAM and normal rats, respectively, using magnetic-bead systems (Miltenyi Biotech, Bergish Gladbach, Germany). The isolated CD4-positive T cells and antigen-presenting dendritic cells were co-cultured in RPMI 1640 (Gibco, Grand Island, NY, USA) and 10% fetal bovine serum (FBS), supplemented with iACS supernatant, recombinant APN (Adipo Bioscience, CA, USA), or recombinant HGF (Institute of Immunology, Tokyo, Japan) for 5 days. Subsequently, 50 μg/ml purified porcine heart myosin was added, and T-cell proliferation was estimated using the Cell Counting Kit-8 (Dojindo, Kumamoto, Japan).[8]

Histology

Myocarditis severity was graded on hematoxylin and eosin (H&E)-stained whole sections (0, no inflammatory infiltrates; 1, small foci of inflammatory cells; 2, larger foci <100 inflammatory cells; 3, more than 10% of a cross-section involved; and 4, more than 30% of a cross-section involved).[11] The CD68-, CD4-, or CD4/Foxp3-positive cells were counted in 5 random fields (magnification: ×600) to assess the infiltration of macrophages, CD4-positive T cells, or Foxp3-positive regulatory T cells, respectively.[8]

Statistical Analysis

Values are given as the mean±SD. All analyses were performed using SPSS 11.0J for Windows (SPSS, Chicago, IL, USA) and the R program.

Detailed methods are presented in **Supplementary File 1**.[9]

Results

Characterization of SVFCS and iACS In Vitro

The characteristics and fundamental behavior of the SVFCS and iACS were compared histologically and biochemically in vitro. The cells in the SVFCS were confluent and spindle-shaped. The cells in iACS were similar but many contained a

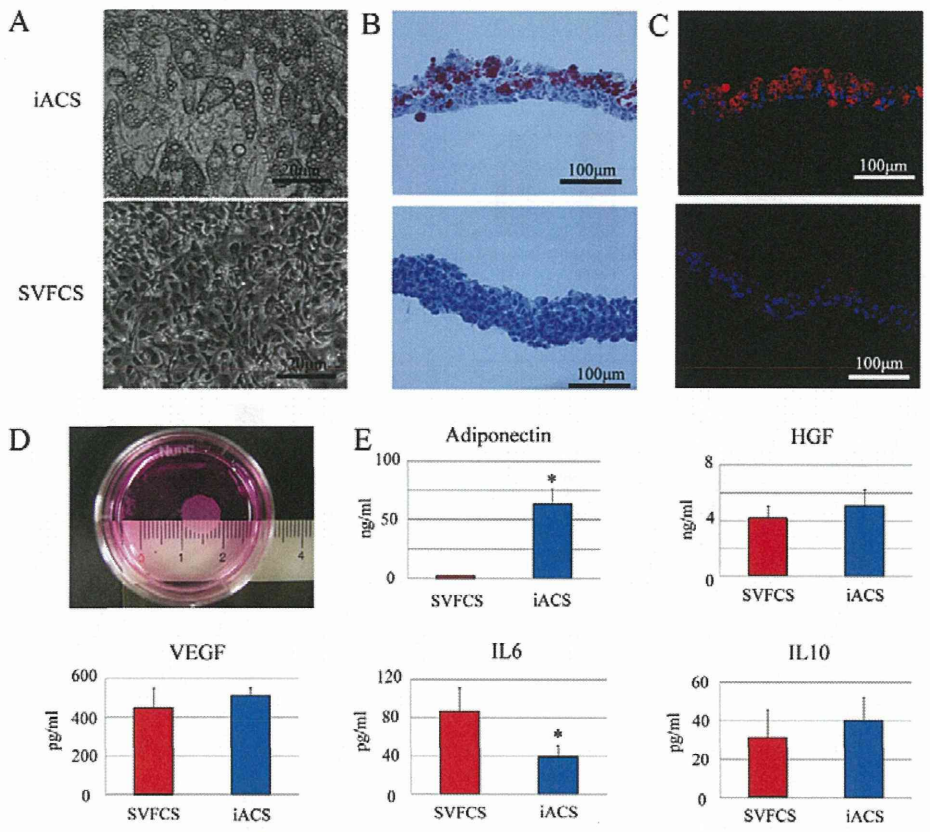

Figure 1. Characterization of the induced adipocyte cell sheet (iACS) in vitro. (**A**) Representative micrographs (**B**) Oil-red O staining. (**C**) Representative immunostaining for adiponectin (APN). Red indicates APN; blue, nuclei (n=7 each). (**D**) iACS detached from the temperature-responsive culture dish. (**E**) APN, hepatocyte growth factor (HGF), vascular endothelial growth factor (VEGF), interleukin (IL)6, and IL10 cytokine levels in cell-sheet supernatants by ELISA analysis (n=7 each). *P<0.05 vs. stromal vascular fraction cell-sheet (SVFCS). There was significantly more released APN in the culture supernatant of iACS than of SVFCS (P<0.001, unpaired t-test).

number of small cytoplasmic vesicles (**Figure 1A**) that stained positive with oil-red O, indicating that the vesicles were fat droplets. Only approximately half the SVF cells had differentiated into adipocytes (**Figure 1B**). Each iACS was approximately 9 mm in diameter and 140-μm thick (**Figure 1D**). Immunohistolabeling revealed that APN was markedly upregulated in the cytoplasm of mature adipocytes in the iACS, but not in the undifferentiated SVF cells in the SVFCS (**Figure 1C**). The amount of extracellularly released APN in vitro was significantly and markedly greater in the culture supernatant of the iACS than in that of the SVFCS (P<0.001), as assessed by enzyme-linked immunosorbent assay (ELISA) (**Figure 1E**). The levels of HGF, vascular endothelial growth factor (VEGF) and anti-inflammatory IL10 were not significantly different between the SVFCS and the iACS, whereas the level of pro-inflammatory IL6 in the iACS culture supernatant was significantly lower (P=0.001).

Inhibition of Antigen-Specific CD4-Positive T-Cell Proliferation by iACS In Vitro

We first examined the expression of 2 different APN receptors (AdipoR1 and AdipoR2) in CD4-positive T cells, CD8-positive T cells and dendritic cells. Using quantitative real-time PCR, we detected similar levels of 2 genes in these 3 cell types (**Figure 2A**).

Next, the effects of iACS transplantation on CD4-positive T-cell-related immunity in the EAM rats were assessed by an antigen-specific T-cell proliferation assay in vitro.

The addition of porcine myosin significantly and markedly increased the proliferation of CD4-positive T cells that were isolated from the spleen of the EAM rats (**Figure 2B**). The addition of recombinant APN and HGF at more than 30 ng/ml and 2 ng/ml, respectively, significantly suppressed the antigen-induced CD4-positive T-cell proliferation (**Figure S1**). The proliferation was diminished significantly more by the addition of an iACS supernatant, compared with 60 ng/ml APN or 5 ng/ml HGF, which were the average amounts released by iACS in vitro (P<0.001 for Myosin (+) vs. APN (60 ng/ml) and HGF (5 ng/ml vs. iACS supernatant). VEGF addition did not have any effect on T-cell proliferation (data not shown). ELISA analysis of the supernatant after incubating the antigen-induced CD4-positive T cells with a specific antigen revealed that adding recombinant APN (60 ng/ml), recombinant HGF (5 ng/ml) or iACS supernatant significantly diminished the release of IFNγ, IL17 and IL6 from the cells (**Figures 2C–E**).

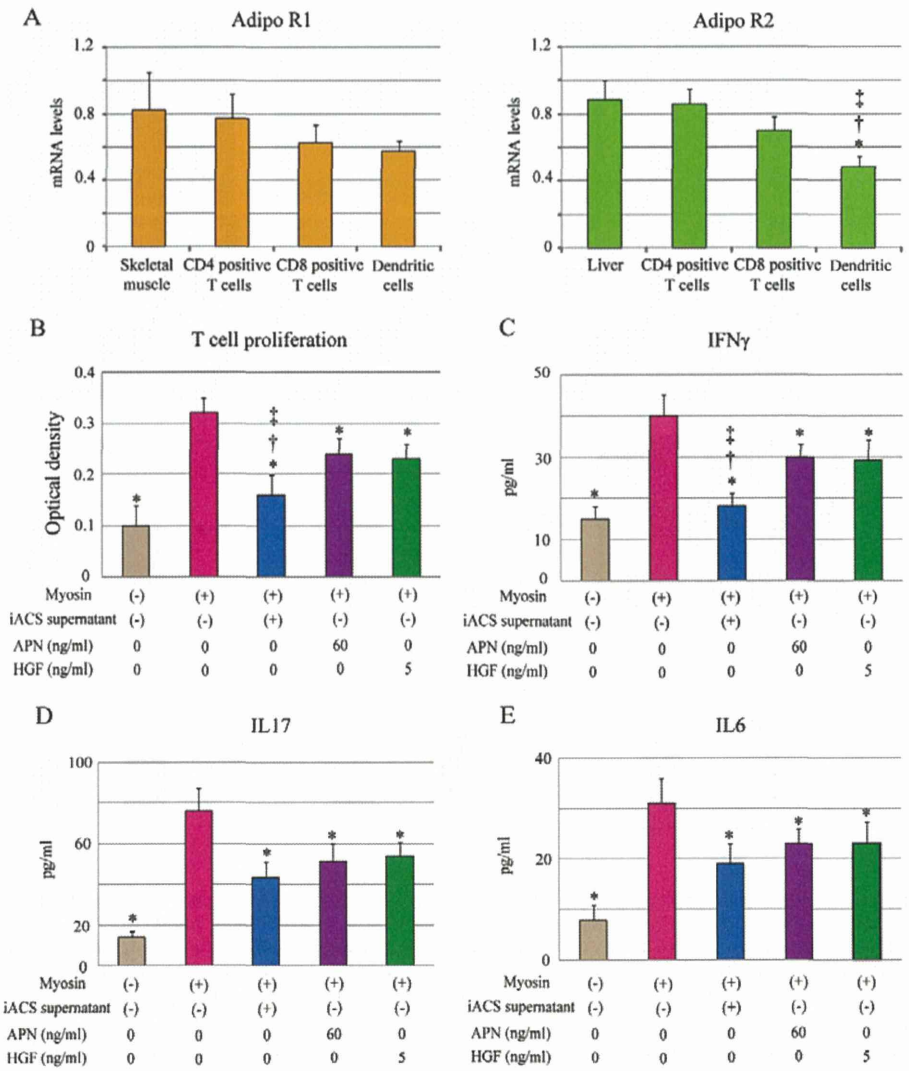

Figure 2. Expression of adiponectin (APN) receptors and CD4-positive T-cell proliferation assay. (**A**) mRNA levels of 2 different APN receptors (AdipoR1 and AdipoR2) in CD4-positive T cells, CD8-positive T cells and dendritic cells (n=7 each, ANOVA). *P<0.05 vs. Liver, †P<0.05 vs. CD4 positive T cells, ‡P<0.05 vs. CD8 positive T cells. All mRNA levels are normalized to GAPDH. (**B–E**) Addition of induced adipocyte cell-sheet (iACS) supernatant, recombinant APN (60 ng/ml) or hepatocyte growth factor (HGF) (5 ng/ml) significantly suppressed the CD4-positive T-cell proliferation (P<0.001) and production of interferon (IFN)γ (P<0.001), interleukin (IL)17 (P<0.001) and IL6 (P<0.001) (n=7 each, ANOVA). *P<0.05 vs. Myosin (+), †P<0.05 vs. APN (60 ng/ml), ‡P<0.05 vs. HGF (5 ng/ml).

Delivery of APN, HGF and VEGF Into EAM Rat Heart by iACS Transplantation

The expression of APN, HGF and VEGF in the EAM rat heart after treatment was assessed by immunohistolabeling and ELISA. Most of the green fluorescent protein (GFP)-positive transplanted cells on day 21 in both the SVFCS and iACS groups remained on the surface of the heart (**Figures 3B,C**), and the number in both engrafted cell sheets gradually decreased from day 8 to day 42 (SVFCS: P=0.026, iACS: P=0.045; **Figure 3J**). Relatively small amounts of APN were detected at the inflamed interstitium and perivascular area in the Sham and SVFCS groups on day 21 (**Figures 3A,B**). In the iACS group, APN expression was higher at the interstitium near the inflammatory cells and the perivascular area, especially in the epicardium near the transplanted iACS.

ELISA showed that the cardiac expression of APN in the inflamed area gradually increased over 42 days in the Sham and SVFCS groups, whereas the iACS transplantation significantly and markedly increased the APN expression compared to the other groups for 21 days; thereafter, high APN expression was maintained through the 42 days of the experiment (APN on day 21: P=0.007 for iACS vs. SVFCS and Sham; **Figure 3G**). Both HGF and VEGF were expressed in the inflamed area, but not in the non-inflamed area, on day 21 as assessed by immunohistolabeling (data not shown); the expression levels of HGF and VEGF on days 21 and 42 were similarly greater in the SVFCS and iACS groups than in the Sham group ([HGF on day 21: P=0.001 for iACS and SVFCS

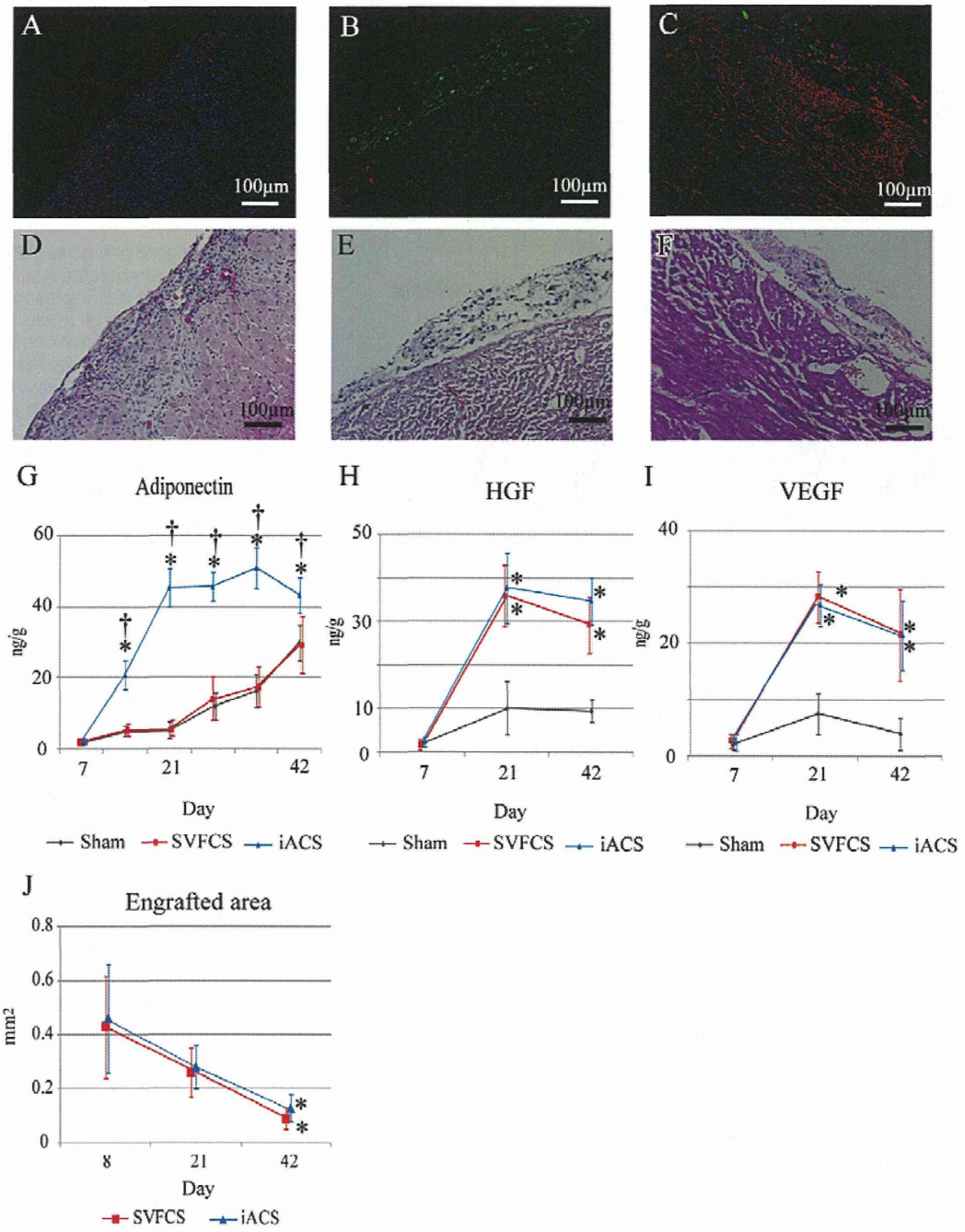

Figure 3. Delivery of cardioprotective factors to the experimental autoimmune myocarditis (EAM) rat heart by induced adipocyte cell-sheet (iACS) transplantation in vivo. (**A**–**C**) Representative immunostaining for adiponectin (APN) 14 days after the Sham operation (**A**), or green fluorescent protein (GFP)-positive stromal vascular-fraction cell-sheet (SVFCS) (**B**) and iACS (**C**) transplantation, respectively. Red, APN; blue, nuclei. (**D**–**F**) Hematoxylin and eosin staining of a serial section from the sample in (**A**), (**B**) and (**C**), respectively. (**G**–**I**) Cardiac expression of APN (**G**), hepatocyte growth factor (HGF) (**H**), and vascular endothelial growth factor (VEGF) (**I**) over time by ELISA (APN: Sham, n=7; SVFCS, n=6; iACS, n=7) (HGF and VEGF: Sham, n=6; SVFCS, n=5; iACS, n=7). *P<0.05 vs. Sham, †P<0.05 vs. SVFCS. (**J**), Quantification of the engrafted GFP-positive cell-sheet area in the iACS and SVFCS groups (n=4 each). *P<0.05 vs. day8.

vs. Sham] [VEGF on day 21: P<0.001 for iACS and SVFCS vs. Sham]) (**Figures 3H,I**).

Induced ACS Transplantation Ameliorates Autoimmune Myocarditis in Rats

The severity of myocarditis in the EAM rats on day 21 was assessed and scored using H&E-stained heart sections (n=12

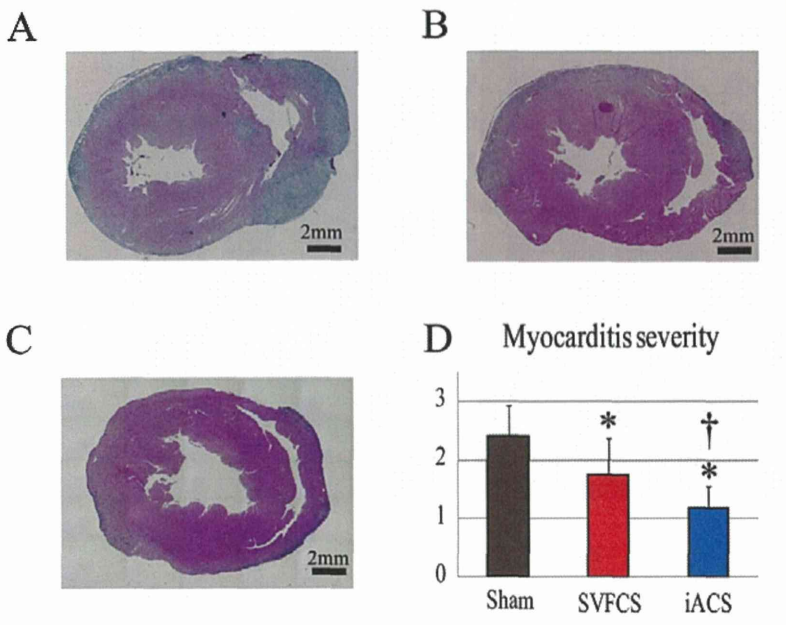

Figure 4. Induced adipocyte cell-sheet (iACS) transplantation ameliorates autoimmune myocarditis in rats. (**A**–**C**) Representative hematoxylin-eosin staining of whole cardiac sections 14 days after a Sham operation (**A**) or stromal vascular-fraction cell-sheet (SVFCS) (**B**) or iACS (**C**) transplantation. (**D**) Myocarditis severity was scored by the degree of inflammatory cell infiltration (n=12 each). The myocarditis severity score was significantly lowest in the iACS group, followed by the SVFCS group, compared to the Sham group (P<0.001, Kruskal-Wallis test). *P<0.05 vs. Sham, †P<0.05 vs. SVFCS.

each).[10] Inflammatory cells with polymorphous nuclei were abundant throughout the sham-treated hearts (**Figure 4A**). The degree of accumulation was globally less in the iACS group, in which it was localized around the blood vessels or near the pericardial tissue, than in the other groups (**Figures 4B,C**). The myocarditis severity score was significantly smallest in the iACS group, followed by the SVFCS group (P=0.001 for iACS vs. SVFCS vs. Sham; **Figure 4D**).

The distribution of accumulated cells that regulate immune reactions, such as macrophages, T cells, and regulatory T cells, was evaluated by immunohistolabeling for CD68, CD4, and CD4/Foxp3, respectively.

The accumulation of CD68-positive macrophages and CD4-positive T cells in the myocardial interstitium was markedly and significantly lower in the iACS group than in the Sham group ([CD68: P<0.001 for iACS vs. SVFCS vs. Sham] [CD4: P<0.001 vs. iACS and SVFCS vs. Sham]) (**Figures 5A,B,D**). Although Foxp3/CD4-double positive regulatory T cells were not abundant in the myocardium of any group, the ratio of Foxp3-positive to CD4-positive T cells was significantly greater in the iACS and SVFCS groups than in the Sham group (P=0.006 for iACS and SVFCS vs. Sham; **Figures 5C–E**).

The levels of molecules that regulate immune reactions or inflammation, such as IFNγ, monocyte chemoattractant protein (MCP)1, tumor necrosis factor (TNF)α, and IL17, in the heart tissue, were significantly lower in the iACS and the SVFCS groups compared to the Sham group, as assessed by using an ELISA (**Figure 5F**).

Reverse LV Remodeling by iACS Transplantation in EAM Rats

Typical histological features of LV remodeling, such as myocyte hypertrophy, capillary density and collagen accumulation, were assessed in the LV of the EAM rats by using H&E staining, immunohistolabeling for CD31, and Masson-trichrome (MT) staining, respectively. On day 42, H&E staining revealed that the myocyte diameter was significantly smaller in the iACS group than in the SVFCS and Sham groups (P<0.001 for iACS vs. SVFCS and Sham) (**Figures 6A,C**). However, there were no significant differences in vascular-capillary density among the 3 groups (**Figure S2**). MT staining of the non-inflamed area showed that the percentage of fibrosis was significantly smaller in the iACS and SVFCS groups than that in the Sham group (iACS, 4.5±2.1; SVFCS, 6.1±2.2; Sham, 21±6%; P<0.001; **Figures 6B,D**). MT-stained whole hearts showed a more severely enlarged LV cavity and thin LV wall in the Sham group compared with the iACS or SVFCS groups.

Quantitative real-time PCR of these samples showed that the expressions of transforming growth factor (TGF)β, metalloproteinases (MMP)2, and MMP9 were significantly lower in the iACS and SVFCS groups compared with the Sham group (**Figure S3**).

Preserved Cardiac Performance by iACS Transplantation in the EAM Rats

Cardiac performance after treatment was evaluated by serial echocardiography every 7 days and by cardiac catheterization on day 42. The hearts of all the groups showed gradually decreased LVEF (**Figure 7A**) and increased RWMI (**Figure 7B**) until day 56. However, the progressive changes in LVEF and RWMI were significantly least severe in the iACS group, followed by the SVFCS group, and then the Sham group (LVEF on day 56: iACS, 56.7±5.0; SVFCS, 46.9±7.2; Sham, 35.3±5.0%; P<0.001 for iACS vs. SVFCS vs. Sham). The hearts of all the groups showed a gradually decreased LV anterior wall diameter (AWD) and enlarged LV end-diastolic dimension (EDD) until day 56. Both LVAWD and LVEDD on day 42 were significantly larger and smaller, respectively, in the iACS and SVFCS groups than in the Sham group (**Figures 7C,D**; LVAWD: P<0.001 for iACS and SVFCS vs. Sham; (LVEDD: P<0.001 for iACS and SVFCS vs. Sham). Cardiac catheterization using a conductance catheter revealed that the end-systolic pressure-volume relationship (ESPVR) was significantly greater in the iACS group than in the Sham group (P<0.001 for iACS vs. SVFCS vs. Sham; **Figure 7E**).

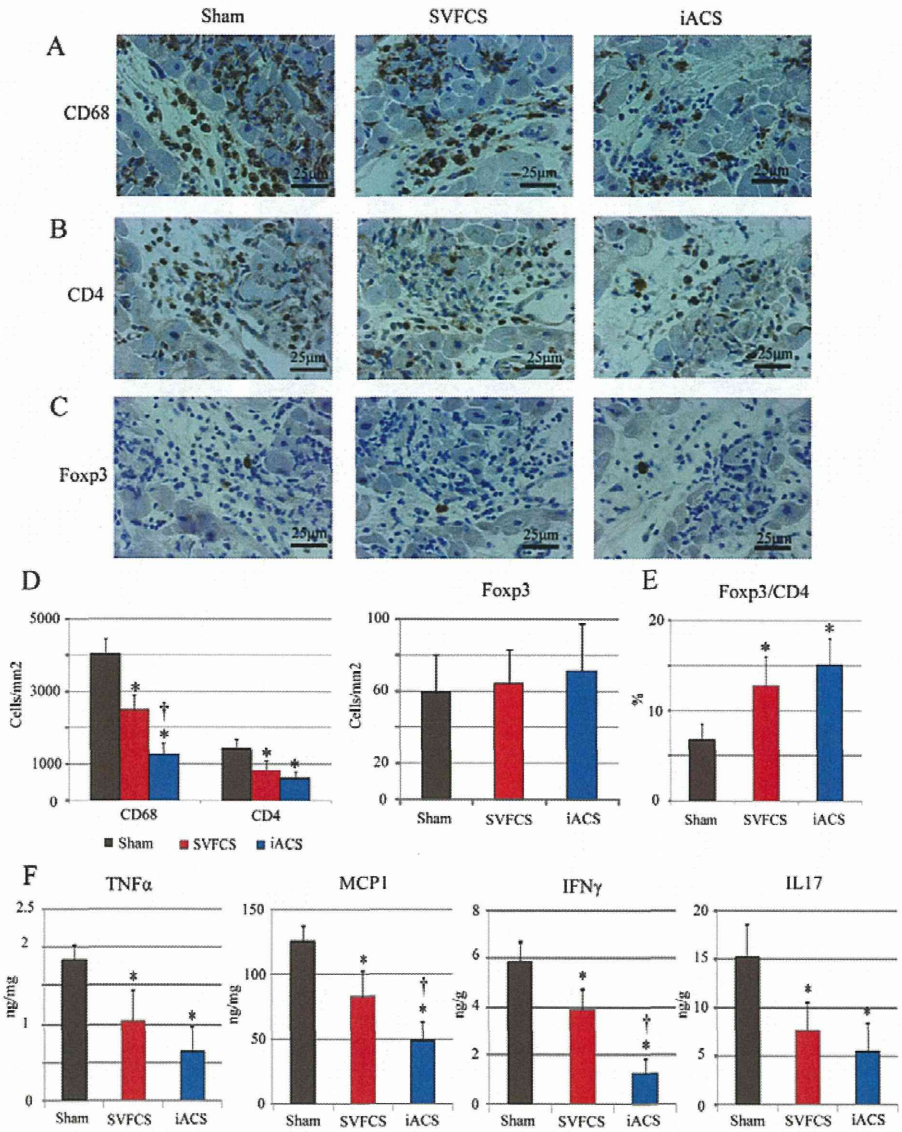

Figure 5. Induced adipocyte cell-sheet (iACS) suppressed the effector T-cell and macrophage responses, and promoted the regulatory T-cell response in experimental autoimmune myocarditis (EAM) rat heart. (**A**–**C**) Representative immunostaining for CD68 (**A**), CD4 (**B**), and Foxp3 (**C**) on postoperative day 14 in each group. (**D**) Quantification of CD68, CD4, and CD4/Foxp3-positive cells (n=12 each). CD68-positive macrophage accumulation in the myocardial interstitium was lowest in the iACS group followed by the stromal vascular-fraction cell-sheet (SVFCS) group compared to the Sham group ($P<0.001$, ANOVA). *$P<0.05$ vs. Sham, †$P<0.05$ vs. SVFCS. (**E**) Ratio of Foxp3-positive regulatory cells to CD4-positive T cells. *$P<0.05$ vs. Sham (n=12 each). (**F**) Myocardial tissues of EAM rat were homogenized and subjected to ELISA to detect tumor necrosis factor (TNF)α, monocyte chemotactic protein (MCP)1, interleukin (IL)17, and interferon (IFN)γ (n=12 each). *$P<0.05$ vs. Sham, †$P<0.05$ vs. SVFCS.

In addition, both dP/dt max and –dP/dt min were significantly greater in the iACS group than in the other groups (**Table S1**).

Discussion

We demonstrated here that iACS, which is generated from SVF isolated from subcutaneous fat tissues, extracellularly released a variety of cardioprotective factors including APN in vitro, and the released factors efficiently inhibited antigen-specific T-cell proliferation via the downregulation of IFNγ, IL17, and IL6 in vitro. Epicardially transplanted iACS supplied greater amounts of cardioprotective factors, such as APN, HGF or VEGF, into the inflamed myocardium of EAM rat hearts for at least 35 days, compared to the SVFCS transplantation or the Sham operation. Consequently, the iACS-transplanted EAM rat hearts showed less severe inflammation, lower expression levels of inflammatory cytokines, and a greater Foxp3-positive regulatory T-cell ratio, compared to the SVFCS-transplanted or Sham-operated EAM hearts. In addition, there was less progression of histological and functional LV remodeling in the EAM hearts following the iACS transplantation than after SVFCS transplantation or the Sham op-